



## CHAPTER IV

### METAL COMPLEXATION VIA BENZOXAZINE-BASED MOLECULES: AN APPROACH OF MEMBRANE ELECTRODE FOR PROTON EXCHANGE MEMBRANE FUEL CELL

#### 4.1 Abstract

*N,N*-bis(2-hydroxy-3,5-dimethylbenzyl)methylamine forms host-guest compound with platinum ions. The inclusion phenomena in solution are confirmed from a new peak at 352 nm as observed by UV-Visible spectroscopy and the peaks shift upon chemical shift values as observed by  $^1\text{H-NMR}$ . The efficiency of platinum ion interaction quantified by Pedersen's technique clarifies the platinum ion extraction is as high as 80%. The single crystal analysis of the product obtained from ion extraction shows the complexation between *N,N*-bis(2-hydroxy-3,5-dimethylbenzyl)methylamine and platinum tetrachloride in solid state under the host-guest ratio of 2:1.

Keyword: Host-guest compound, Benzoxazine, Catalyst, Membrane electrode assembly, Proton exchange membrane fuel cell

## 4.2 Introduction

Fuel cells are electrochemical devices that directly convert chemical energy into electrical energy, heat and water. Among various types of fuel cells, polymer electrolyte membrane fuel cell (PEMFC) is the most promising candidate system as it can be power source in different applications ranging from portable power supplies stationary ones. There are several advantages of PEMFC including high efficiency, low operating temperature (70-90°C), rapid start-up and fuel flexibility.

In general, Pt-based electrocatalyst is needed either in anode for H<sub>2</sub> oxidation or in cathode for O<sub>2</sub> and air reduction in PEMFC. However, many problems still remain such as the low utilization and poor substrate adherence.<sup>1</sup> The main problem in PEMFC is the ineffective distribution of precious metal in catalyst layer.<sup>2</sup> This reduces the performance of fuel cell because of the limited utilization of Pt particles. Finding new direction to improve catalytic efficiency and lower catalytic loading are critically important for PEMFC development.

In order to enhance the Pt utilization and reduce Pt-loadings in electrocatalyst, numerous approaches have been intensively investigated. The approaches are for example, introducing new catalyst-supporting materials to maximize Pt activity,<sup>3</sup> using Pt-alloy electrocatalyst<sup>4</sup> and developing new electrocatalysts to substitute Pt.<sup>5</sup> The purpose of this work is to investigate a new approach of membrane electrode with supramolecular structured catalyst layer.

As we already demonstrated benzoxazine dimer as a novel host molecule on which copper ion is entrapped through coordinate network,<sup>6</sup> the present work aims to show the system where Pt is deposited in the framework. The supramolecular structured catalyst at the interface is a good model to propose novel membrane electrode with several advantages such as the precise active site, the prevention of catalyst agglomeration, and the distribution of the catalyst on the surface. This leads us to an effective way to initiate the function of the catalyst in the membrane electrode assembly (MEA). In this work, we propose our original idea by showing how complexation of *N,N*-bis(2-hydroxy-3,5-dimethylbenzyl)methylamine with Pt ions is possible.

## 4.3 Experimental

### 4.3.1 Materials

All chemicals were reagent grade and used without further purification. 2,4-Dimethylphenol, paraformaldehyde and methylamine were purchased from Merck, Germany. Chloroform-*d* was purchased from Aldrich, Germany. Anhydrous sodium sulfate and sodium hydroxide were obtained from Carlo Erba, Italy. Potassium tetrachloroplatinate ( $K_2PtCl_4$ ), isopropanol and chloroform were from Wako, Japan. Diethyl ether and 1,4-dioxane were purchased from Labscan, Ireland.

### 4.3.2 Instruments and Equipment

#### 4.3.2.1 Fourier Transform Infrared (FTIR) Spectrophotometer

Fourier transform infrared (FTIR) spectra were recorded by using a Nicolet Spectrophotometer with 32 scans at a resolution of  $2\text{ cm}^{-1}$ . A frequency range of  $4000\text{--}400\text{ cm}^{-1}$  was observed by using deuterated triglycerinesulfate detector (DTGS) with specific detectivity of  $1 \times 10^9\text{ cm}\cdot\text{Hz}^{1/2}\cdot\text{w}^{-1}$ .

#### 4.3.2.2 Nuclear Magnetic Resonance (NMR)

NMR spectra were obtained from a Varian Mercury 400 MHz spectrometer (USA). The deuterated solvent used was  $CDCl_3$ . The internal reference for  $^1H$ -NMR was tetramethylsilane.

#### 4.3.2.3 X-ray Diffractometer

Single crystal analysis was collected by a Rigaku RAXIS RAPID diffractometer with a graphite monochromated  $Mo\text{-}K_\alpha$  radiation at 296 K. The structure was solved by direct methods (SIR92) and refined by full-matrix least-squares on  $F^2$  with RAPID AUTO program. All non-hydrogen atoms were refined with anisotropic displacement parameters.

#### 4.3.2.4 UV-Vis Spectrophotometer

UV-Visible spectra were measured by a Shimadzu UV-2550 UV-Vis spectrophotometer. The samples were dissolved in chloroform.

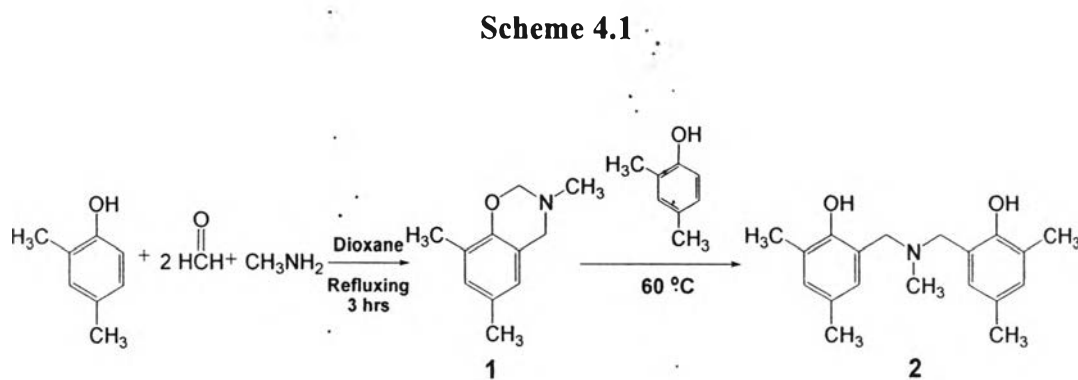
#### 4.3.2.5 Electrospray Ionization Mass Spectroscopy

Electrospray ionization mass spectrometry (ESIMS) was recorded by using a MicroTOF LC, Bruker instrument equipped with Bruker Daltonics DataAnalysis 3.3

software with positive mode. Samples were dissolved in chloroform. The capillary voltage was set at 100.0 V.

### 4.3.3 Methodology

*N,N*-bis(2-hydroxy-3,5-dimethylbenzyl)methylamine, **2** was prepared as reported elsewhere<sup>6</sup> and used as a model compound. 3,4-Dihydro-3,6,8-trimethyl-2*H*-1,3-benzoxazine, **1** and 2,4-dimethylphenol (1:1) were mixed and stirred at 60 °C. The mixture was allowed to react until viscous and left for precipitation. The precipitate obtained was collected and washed with diethyl ether before drying. Compound **2** was recrystallized in isopropanol before use. Scheme 4.1 shows the preparation of benzoxazine-based **1** and **2**.



### Complexation in Solution

Solutions of **2** in chloroform and potassium tetrachloroplatinate ( $K_2PtCl_4$ ) in deionized water were prepared. The two solutions were mixed and the mixture was left for a week. The chloroform phase was collected and dried by anhydrous  $Na_2SO_4$  for overnight. The solution was left for crystallization before characterization by UV-Vis spectroscopy,  $^1H$ -NMR, and Electrospray Ionization Mass Spectroscopy (ESIMS).

### Percentage of Metal Ion Extraction

Solutions of  $K_2PtCl_4$  in deionized water ( $0.5 \times 10^{-4}$  M) and **2** in chloroform ( $2.0 \times 10^{-4}$ ,  $1.5 \times 10^{-4}$ ,  $1.0 \times 10^{-4}$ ,  $0.5 \times 10^{-4}$ ,  $0.25 \times 10^{-4}$ ,  $0.125 \times 10^{-4}$ ,  $0.0625 \times 10^{-4}$  and

0.005 x 10<sup>-4</sup> M) were prepared. Each solution was mixed together, vigorously shaken for 1 min, and left for 2 days before analyzing the chloroform phase by UV-Vis spectroscopy. The new peak at 352 nm was measured and calculated for extraction percentage using eq. 1.

$$\% \text{ Extraction} = [(A - A_0)/A] \times 100 \quad \text{eq. 1}$$

where  $A$  is the absorbance after extraction and  $A_0$  is initial absorbance.

#### Single Crystal of Host-Metal Ion Complex

Solutions of **2** in chloroform and K<sub>2</sub>PtCl<sub>4</sub> in deionized water were prepared, vigorously mixed, and left for a week. The organic phase was collected and left until the yellow crystals were obtained. The crystals were used for single crystal analysis and FTIR measurement.

#### 4.4 Results and Discussion

Previously, we reported that **2** showed inclusion phenomena with Cu ion, which can be easily identified by the new peak in UV-Vis spectra.<sup>7</sup> Figure 4.1 shows UV-Vis spectra in chloroform phase of **2** as compared with the solution of **2** after extraction with K<sub>2</sub>PtCl<sub>4</sub> in deionized water.

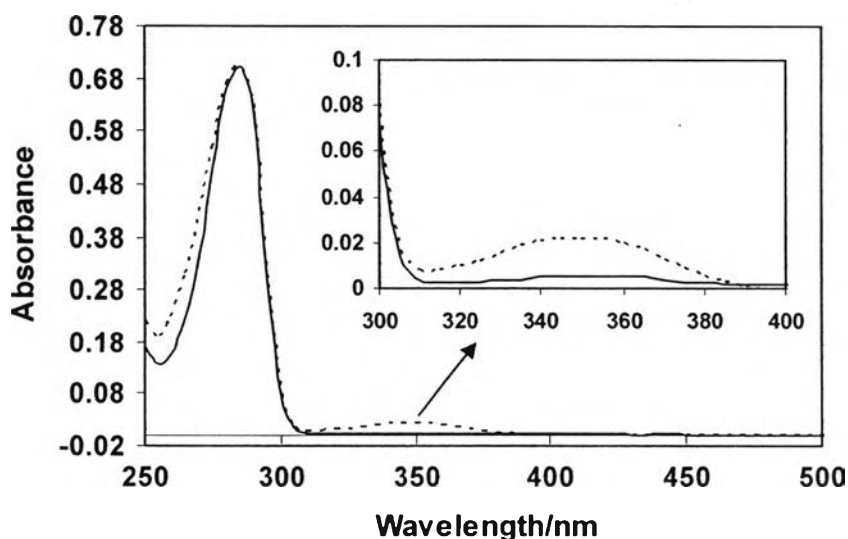


**Figure 4.1** UV-Vis spectra of **2** in chloroform; before extraction (solid line), and after extraction (dotted line).

Compound **2** gives a maximum peak at 285.8 nm. However, after extraction, a new peak at 352 nm is observed implying that **2** acts as a host to form an inclusion phenomena with  $\text{K}_2\text{PtCl}_4$ .

To evaluate the efficiency of platinum ion interaction, liquid-liquid extraction containing aqueous platinum ions and **2** in chloroform was studied. The highest extraction percentage is up to 80% (Figure 4.2).

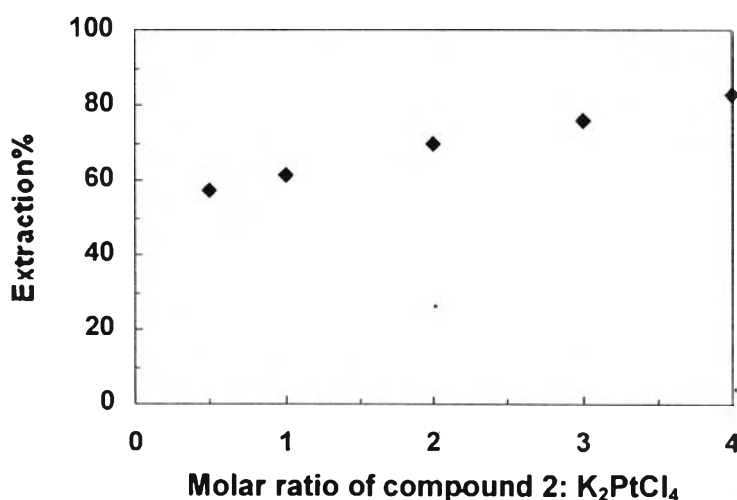


**Figure 4.2** Job plots of **2** and  $\text{K}_2\text{PtCl}_4$ .

$^1\text{H-NMR}$  was applied to confirm the complexation in solution. As shown in Figure 4.3, after extraction **2** with aqueous solution of  $\text{K}_2\text{PtCl}_4$ , the peak of  $\text{CH}_2\text{-N}$  ( $\text{H}_c$ ) is significantly deshielded by 0.07 ppm. The peak ( $\text{H}_b$ ) at 2.15 ppm ( $\text{CH}_3\text{-N}$ ) is shifted to 2.20 ppm. The shifting of these peaks involves the position changes in the cases of methylene ( $\text{CH}_2\text{-N}$ ) and methyl protons ( $\text{CH}_3\text{-N}$ ) of the aza group. This implies that the aza group donates electrons to the metal ions resulting in decreasing the electron density of those protons attached on the aza group when host-guest system was formed.

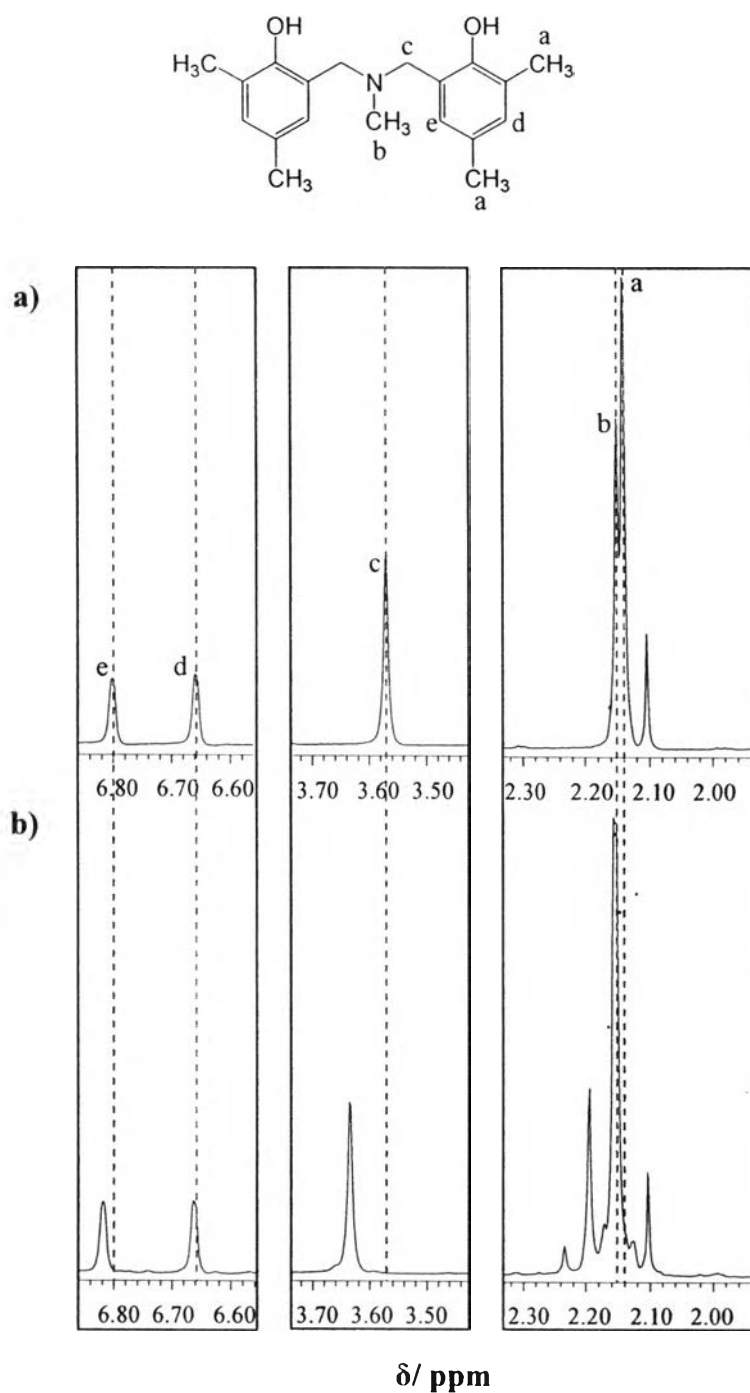


**Figure 4.3**  $^1\text{H}$ -NMR spectra of **2** a) before extraction, and b) after extraction with aqueous solution of  $\text{K}_2\text{PtCl}_4$ .

In order to confirm the inclusion phenomena of the host-guest system, ESIMS was also studied. It can be expected that after extraction of **2** with aqueous solution of  $\text{K}_2\text{PtCl}_4$ , the molecular weight of the complex might increase from

299  $m/z$  to the molecular weight of the complex ( $\sim 935$   $m/z$ ). Unfortunately, the results (Figure 4.4) show that the peaks (M+H) before and after extractions were at  $m/z \sim 300$  which represents the molecular weight of **2**. This might be due to the interaction of the host and guest not strong enough in solution state.

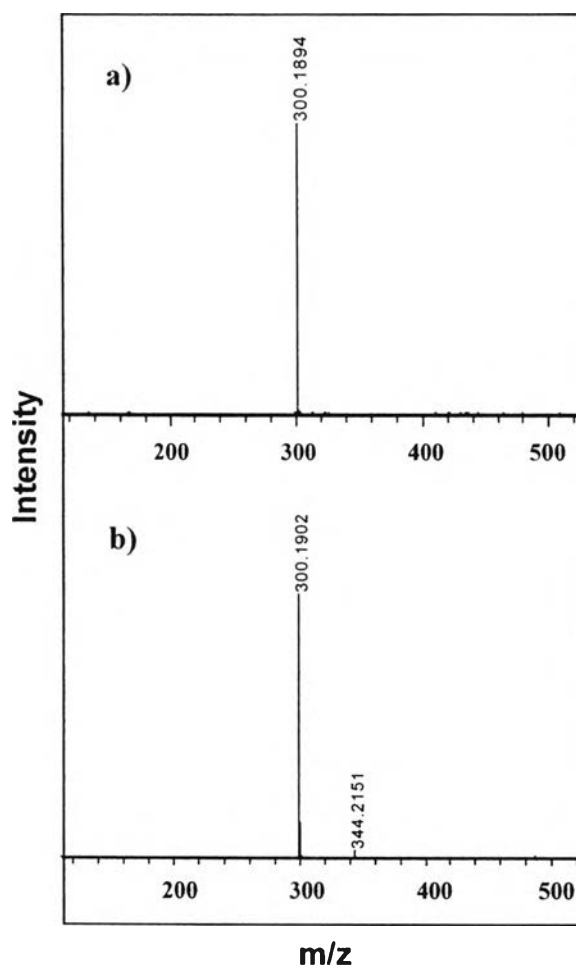


**Figure 4.4** Mass spectra of **2** a) before extraction, and b) after extraction with aqueous solution of  $K_2PtCl_4$ .

In order to study the inclusion phenomena in the solid state, the liquid-liquid extraction of **2** in chloroform and  $K_2PtCl_4$  in aqueous was carried out. The chloroform phase was collected and the solvent was removed. The crude product was recrystallized by  $CHCl_3$  before analyzing by FTIR. A significant change after the extraction especially at the OH bonding region around  $3000-3500$   $cm^{-1}$



belonging to intermolecular hydrogen bonding is observed (Figure 4.5). This indicated that the structure of the host is altered after extraction.

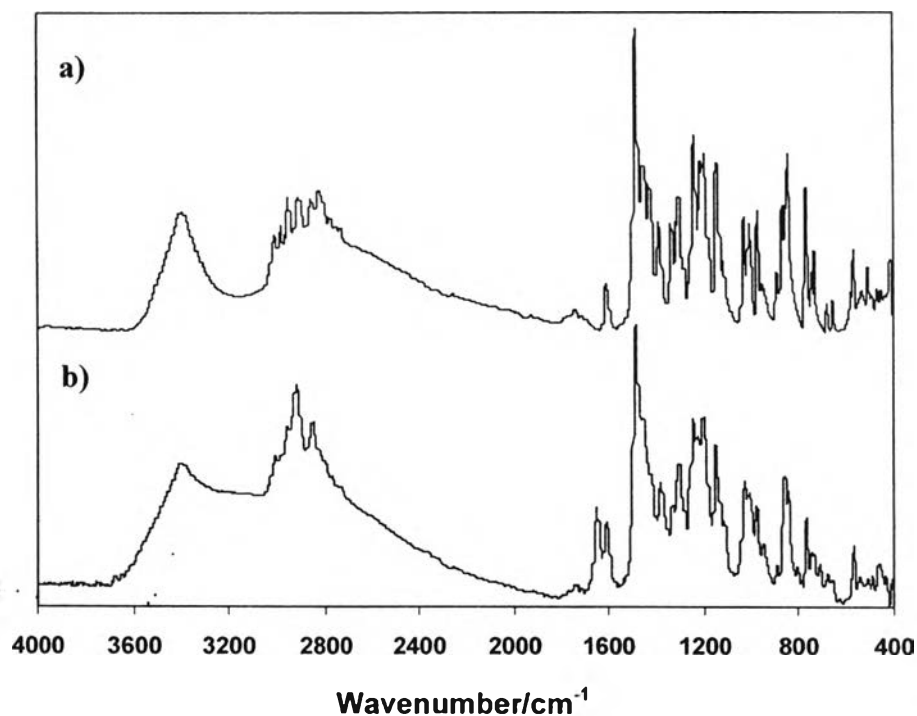


**Figure 4.5** FTIR spectra of **2** a) before extraction, and b) after extraction with aqueous solution of  $\text{K}_2\text{PtCl}_4$ .

The single crystal analysis was further carried out. It is important to note that **2** gave colorless needle-like crystals whereas the extracted solution of **2** and  $\text{K}_2\text{PtCl}_4$  gave yellowish needle-like crystals. Table 4.1 summarizes the X-ray data which confirms the significant change of the unit cell and volume after host-guest complex is formed. Figures 4.6 and 4.7 show the structural analysis of **2** and **2**- $\text{PtCl}_4$  obtained from single crystal analysts using RAPID AUTO program.

**Table 4.1** Crystallographic data of **2** and **2-PtCl<sub>4</sub>** compound

Empirical formula	C <sub>19</sub> H <sub>25</sub> O <sub>2</sub> N	C <sub>19</sub> H <sub>25</sub> O <sub>2</sub> NC <sub>2</sub> Pt <sub>0.5</sub>
Formula weight	299.41	467.86
Temperature (K)	296(1)	296(1)
Wavelength (Å)	0.71075	0.71075
Crystal system	Monoclinic	Monoclinic
Space group	C2 (#5)	P2 <sub>1</sub> /n (#14)
Unit cell dimensions		
a (Å)	23.618(10)	14.61(4)
b (Å)	5.972(2)	8.499(18)
c (Å)	16.806(9)	17.37(3)
β (°)	133.585(13)	111.97(8)
Volume (Å <sup>3</sup> )	1717.0(12)	2000.7(78)
Z	4	4
ρ <sub>calc</sub> (g/cm <sup>3</sup> )	1.158	1.553
μ (cm <sup>-1</sup> )	0.742	37.992
Max. and min. transmission	0.993 and 0.971	0.684 and 0.408
Crystal size (mm <sup>3</sup> )	0.80 X 0.30 X 0.10	0.20 x 0.10 x 0.10
Reflections collected	1226	2625
Independent reflections	409 [R <sub>(int)</sub> = 0.047]	616 [R <sub>(int)</sub> = 0.221]
Observed reflections [ <i>I</i> > 2σ( <i>I</i> )]	7103	1230
Goodness-of-fit on <i>F</i> <sup>2</sup>	0.835	0.873
Final <i>R</i> indices [ <i>I</i> > 2σ( <i>I</i> )]	<i>R</i> 1 = 0.0617 ω <i>R</i> 2 = 0.1651	<i>R</i> 1 = 0.0780 ω <i>R</i> 2 = 0.1919
Largest diff. peak and hole (eÅ <sup>-3</sup> )	1.37 and -0.95	2.47 and -1.48

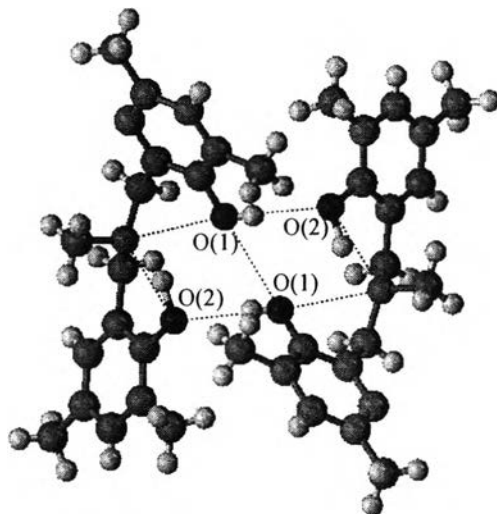


**Figure 4.6** Crystal structure of **2**.

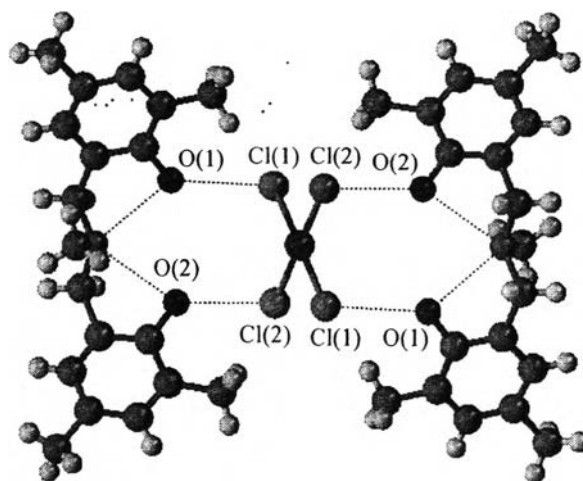


**Figure 4.7** Crystal structure of **2** with  $\text{PtCl}_4$ .

Phongtamrag *et al.*, reported that the supramolecular structure of HBA with copper ion was under the double oxygen-bridged system with the host-guest ratio 1:1.<sup>6</sup> Here, the different host-guest framework is clarified. The framework of **2** might be difficult to maintain resulting in changing the host-guest ratio from 1:1 to 2:1 as well as the hydrogen and coordinate bonds. Moreover, the distance of O(1)-O(2) is changed from 2.895 Å to 7.141 Å after  $\text{PtCl}_4$  inclusion. This results show the destruction of the intermolecular hydrogen bond between HBAs and the formation of halogen bond between HBAs and  $\text{PtCl}_4$ . This complex information is

supported by the change of infrared absorption band related to intermolecular hydrogen bonding from spectrum a to spectrum b in Figure 4.5 and the peak shift in  $^1\text{H-NMR}$  from spectrum a to spectrum b in Figure 4.3.

#### 4.5 Conclusions

The complexation of *N,N*-bis(2-hydroxy-3,5-dimethylbenzyl)methylamine with platinum tetrachloride ion was formed as proved from a new peak at 352 nm observed by UV-Visible spectroscopy. The single crystal analysis confirmed that the framework of the host was changed from inter- and intramolecular hydrogen bonding to intermolecular hydrogen bonding and halogen bond after the complex with the guest was formed with the host-guest ratio 2:1. The changes of infrared absorption band in FTIR and the peak shift in  $^1\text{H-NMR}$  also supported the complex formation.

#### 4.6 Acknowledgements

The authors would like to acknowledge the Thailand Government Research Budget (National Research Council of Thailand), the NRCT-JSPS joint research program (National Research Council of Thailand and Japan Society for Promotion of Science), the Engineering Research and Development Project (National Metal and Materials Technology Center, Thailand), and Research Task Force on Fuel Cell Program (Chulalongkorn university) for research funds. One of the authors, A.P., would like to extend her appreciation the scholarship from Development and Promotion of Science and Technology Talents Project (DPST). Last but not least, the appreciations are extended to Prof. Kohji Tashiro, Toyota Technological Institute, Japan for the X-ray single crystal analysts.

#### 4.7 References

- (1) Colón-Mercado, H. R.; Popov, B. N. *J. Power Sources* **2006**, *155*, 253.
- (2) O'Hayre, R.; Lee, S.; Cha, S.; Prinz, F. B. *J. Power Sources* **2002**, *109*, 483.
- (3) Liu, Z.; Gan, L. M.; Hong, L.; Chen, W.; Lee, J. Y. *J. Power Sources* **2005**, *139*,

- (4) Choi, J. H.; Park, K. W.; Park, I. S.; Nam, W. H.; Sung, Y. E. *Electrochim. Acta* **2004**, *50*, 787.
- (5) Savastenko, N. A.; Brüser, V.; Brüser, M.; Anklam, K.; Kutschera, S. *J. Power Sources* **2007**, *165*, 24.
- (6) Phongtamrug, S.; Tashiro, K.; Miyata, M.; Chirachanchai, S. *J. Phys. Chem.* **2006**, *110*, 21365.
- (7) Phongtamrug, S.; Pulpoka, B.; Chirachanchai, S. *Supramol. Chem.* **2004**, *16*, 269.